Spike timing-dependent plasticity as the origin of the formation of clustered synaptic efficacy engrams

Nicolangelo Libero Iannella[1,2,3]*, Thomas Launey[1] and Shigeru Tanaka[4]

[1] *Launey Research Unit for Molecular Neurocybernetics, RIKEN Brain Science Institute, Wako-shi, Saitama, Japan*
[2] *School of Electrical and Electronic Engineering, The University of Adelaide, Adelaide, SA, Australia*
[3] *Theoretical and Experimental Neurobiology Unit, Okinawa Institute of Science and Technology, Kunigami, Okinawa, Japan*
[4] *Department of Information and Communications Engineering, The University of Electro-Communications, Chofu-shi, Japan*

Edited by: Wulfram Gerstner, Ecole Polytechnique Fédérale de Lausanne, Switzerland

Reviewed by: Claudia Clopath, Ecole Polytechnique Fédérale de Lausanne, Switzerland
Robert Legenstein, Graz University of Technology, Austria

*Correspondence: Nicolangelo Libero Iannella, Launey Research Unit for Molecular Neurocybernetics, RIKEN Brain Science Institute, 2-1 Hirosawa, Wako-shi, Saitama 351-0198, Japan.
e-mail: nicolang@brain.riken.jp

Received: 08 March 2010; Paper pending published: 01 April 2010; Accepted: 14 June 2010; published online: 13 July 2010.

Citation: Iannella NL, Launey T and Tanaka S (2010) Spike timing-dependent plasticity as the origin of the formation of clustered synaptic efficacy engrams. *Front. Comput. Neurosci.* **4**:21. doi: 10.3389/fncom.2010.00021

THE LAYER 2/3 PYRAMIDAL CELL MODEL PARAMETERS

The biophysical model of a reconstructed layer 2/3 pyramidal cell was simulated using NEURON where ion channels were included throughout the axon, soma and dendrites. The types of ionic currents and their respective distributions used in the simulations are based upon available experimental data, mostly from rat, or those used in previous modeling studies (Moczydlowski and Latorre, 1983; Rhodes and Gray, 1994; Mainen et al., 1995; Mainen and Sejnowski, 1996; Rhodes and Llinás, 2001; Poirazi et al., 2003a; Traub et al., 2003; Kampa and Stuart, 2006). The simulations were performed at a nominal temperature of 37°C. When necessary, original rates were adjusted from their original amounts to 37°C using a Q_{10} value, otherwise channel kinetics were not altered. Parameter values of conductance densities used in the simulation are given in **Table 1.** Their descriptions are given below.

Table 1 | Table of conductance parameters and distributions used in simulations.

Symbol	Density (pS/μm²)
DENSITIES USED IN THE LAYER 2/3 PYRAMIDAL CELL MODEL	
g_{L}	Before addition of spines 0.25; After addition of spines 0.3827
g_{Na}	45
g_{K}	68
$g_{K(A)}$	50
$g_{K(H)}$	Monotonically increasing
$g_{Ca(HVA)}$	Monotonically increasing
$g_{Ca(T)}$	4
$g_{Ca(N)}$	Monotonically increasing
$g_{K(Ca)}$	40
g_{K_M}	3.5
g_{mAHP}	15
g_{sAHP}	1.5

$$\beta \quad \begin{array}{l} 35 \quad 9 \\ 0\ 124 \quad 35 \\ 1 \quad 35 \quad 9 \end{array}$$

$$\frac{-h}{\tau_h(V)}$$

$$\alpha_h(V) = \frac{0.024(V+50)}{1-\exp(-(V+50)/5)}$$

$$\beta_h(V) = \frac{-0.0091(V+75)}{1-\exp((V+75)/5)}$$

$$h_\infty(V) = \frac{1}{1+\exp((V+65)/6.2)}$$

$$\tau_h(V) = \frac{1}{\alpha_h(V)+\beta_h(V)}$$

The values for the rates were adjusted from their original values given at 23°C to 37°C using a Q_{10} of 2.3 (Mainen et al., 1995; Mainen and Sejnowski, 1996).

Potassium current I_K

$$I_K = \bar{g}_K n(E_{Kdr} - V)$$
$$\frac{\partial n}{\partial t} = \alpha_n(V)(1-n) - \beta_n(V)n$$
$$\alpha_n(V) = \frac{0.02(V-20)}{1-\exp(-(V-20)/9)}$$
$$\beta_n(V) = \frac{-0.002(V-20)}{1-\exp((V-20)/9)}$$

The values for the rates were adjusted from their original values given at 23°C to 37°C using a Q_{10} of 2.3 (Mainen et al., 1995; Mainen and Sejnowski, 1996).

Transient potassium A-current $I_{K(A)}$

$$I_{K(A)} = \bar{g}_{K(A)} mh(E_{K(A)} - V)$$
$$\frac{\partial m}{\partial t} = \frac{m_\infty(V) - m}{\tau_{m_{K(A)}}(V)}$$
$$\frac{\partial h}{\partial t} = \frac{h_\infty(V) - h}{\tau_{h_{K(A)}}(V)}$$
$$m_\infty(V) = \frac{1}{1+\exp(-(V+0.8)/11.6)}$$
$$h_\infty(V) = \frac{1}{1+\exp((V+51.3)/7.9)}$$
$$\tau 2(V) = \frac{\beta_m(V)}{0.031(1+\alpha_m(V))}$$
$$\tau_{m_{K(A)}}(V) = \min(\tau 2(V), \tau_{min})$$
$$\tau_{h_{K(A)}}(V) = \frac{\beta_h(V)}{0.001364(1+\alpha_h(V))}$$
$$\alpha_m(V) = \exp(0.03(V+60))$$
$$\beta_m(V) = \exp(0.015(V+60))$$
$$\alpha_h(V) = \exp(0.01(V-40))$$
$$\beta_h(V) = \exp(0.008(V-40))$$

The values for the rates were adjusted from their original values given at 22–37°C using a Q_{10} of 3 (Zhou and Hablitz, 1996). Steady state activation and inactivation were identical to those previously reported for Layer 2/3 cells (Zhou and Hablitz, 1996), however time constants were modified in order to better fit both the frequency dependence and the extent of dendritic regenerative events (Kampa and Stuart, 2006; Larkum et al., 2007), since it has been previously reported that $I_{K(A)}$, along with calcium influx via activation of voltage-dependent calcium channels, can play a critical role in dendritic electrogenesis (Kampa and Stuart, 2006).

Potassium H-current $I_{K(H)}$

$$I_{K(H)} = \bar{g}_{K(H)} m(E_{K(H)} - V)$$
$$\frac{\partial m}{\partial t} = \frac{m_\infty(V) - m}{\tau_{m_{K(H)}}(V)}$$
$$m_\infty(V) = \frac{1}{1+\exp((V+75)/5.5)}$$
$$\tau_{m_{K(H)}}(V) = \frac{1}{\exp(-0.086V - 14.6) + \exp(-1.87 + 0.07V)},$$

The channel kinetics for the *h*-current was taken without modification from Traub et al. (2003).

High-Voltage-Activated (HVA) L-type calcium current $I_{Ca(HVA)}$

$$I_{Ca(HVA)} = \bar{g}_{Ca(HVA)} m^2 h([Ca]_i)(\mathcal{E}_{Ca(HVA)} - V)$$
$$\mathcal{E}_{Ca(HVA)} = \frac{R\mathcal{T}}{2\mathcal{F}} \ln\left(\frac{[Ca]_o}{[Ca]_i}\right)$$
$$\frac{\partial m}{\partial t} = \alpha_m(V)(1-m) - \beta_m(V)m$$
$$\frac{\partial h}{\partial t} = \frac{h_\infty(V,[Ca]_i) - h}{\tau_{h_{Ca(HVA)}}}$$
$$\alpha m(V) = \frac{1.6}{1+\exp(-0.072(V-5))}$$
$$\beta_m(V) = \frac{-0.02(V+8.9)}{1-\exp((V+8.9)/5)}$$
$$h_\infty(V,[Ca]_i) = \left(\frac{2\mu M}{2\mu M + [Ca]_i}\right)\frac{1}{(1+\exp((V+42)/8)}$$
$$\tau_{h_{Ca(HVA)}} = 200$$

The values for the rates were slightly adjusted from their original values given at 34°C to 37°C using a Q_{10} of 2.3 (Rhodes and Gray, 1994; Traub et al., 2003).

Low-Voltage-Activated T-type calcium current $I_{Ca(T)}$

$$I_{Ca(T)} = \bar{g}_{Ca(T)} m^2 h(E_{Ca(T)} - V)$$
$$\frac{\partial m}{\partial t} = \frac{m_\infty(V) - m}{\tau_{m_{Ca(T)}}(V)}$$
$$\frac{\partial h}{\partial t} = \frac{h_\infty(V) - h}{\tau_{h_{Ca(T)}}(V)}$$
$$m_\infty(V) = \frac{1}{1+\exp(-(V+45)/7.4)}$$
$$h_\infty(V) = \frac{1}{1+\exp((V+65)/5)}$$
$$\tau_{m_{Ca(T)}} = 3 + \frac{1}{\exp((V+50)/20) + \exp(-(V+125)/15)}$$
$$\tau_{h_{Ca(T)}} = 30 + \frac{1}{\exp((V+56/4) + \exp(-(V+415)/50)}$$

The channel kinetics for T-type calcium was taken from Kampa et al. (2006) without modification.

High-Voltage-Activated N-type calcium current $I_{\mathrm{Ca(N)}}$

$$I_{\mathrm{Ca(N)}} = \bar{g}_{\mathrm{Ca(N)}} m^2 h \,\mathrm{GHK}(V,[\mathrm{Ca}]_i,[\mathrm{Ca}]_o)$$

$$\mathrm{GHK}(V,[\mathrm{Ca}]_i,[\mathrm{Ca}]_o) = -x\left(1-\frac{[\mathrm{Ca}]_i}{[\mathrm{Ca}]_o}\mathrm{e}^{\frac{V}{x}}\right) f\left(\frac{V}{x}\right)$$

$$x = 0.0853\frac{\mathcal{T}}{2},\ f(z) = \begin{cases} \frac{z}{\mathrm{e}^z-1} & \text{if abs(z)} \geq 10^{-6} \\ 1-\frac{z}{2} & \text{otherwise} \end{cases}$$

$$\frac{\partial m}{\partial t} = \alpha_m(V)(1-m) - \beta_m(V)m$$

$$\frac{\partial h}{\partial t} = \frac{h_\infty(V)-h}{\tau_{h_{\mathrm{Ca(N)}}}}$$

$$\alpha_m(V) = \frac{0.1967(V-19.88)}{1-\exp(-(V-19.88)/10)}$$

$$\beta_m(V) = 0.046\exp(-V/20.73)$$

$$\alpha_h(V) = 0.00016\exp(-V/48.4)$$

$$\beta_h(V) = \frac{1}{1+\exp(-(V-39)/10)}$$

$$m_\infty(V) = \frac{\alpha_m(V)}{\alpha_m(V)+\beta_m(V)}$$

$$h_\infty(V) = \frac{\alpha_h(V)}{\alpha_h(V)+\beta_h(V)}$$

$$\tau_{m_{\mathrm{Ca(N)}}} = \frac{1}{\alpha_m(V)+\beta_m(V)}$$

$$\tau_{h_{\mathrm{Ca(N)}}} = \frac{1}{\alpha_h(V)+\beta_h(V)}$$

The channel kinetics was taken from Lazarewicz et al. (2002) with the temperature set to 37°C and where $\mathcal{F}$ = 96485 C mol^{-1} is Faraday's constant, R = 8.1345 J°K^{-1}mol^{-1} is the gas constant, and $\mathcal{T}$ denotes absolute temperature in °K (degrees kelvin).

Calcium gated potassium current $I_{\mathrm{K(Ca)}}$

$$I_{\mathrm{K(Ca)}} = \bar{g}_{\mathrm{K(Ca)}} m(E_{\mathrm{K(Ca)}} - V)\min([Ca]_i/2(\mu\mathrm{M}),1)$$

$$\frac{\partial m}{\partial t} = \alpha_m(V)(1-m) - \beta_m(V)m$$

$$\alpha_m(V) = \begin{cases} 2/37.95\exp\big((V+50)/11-(V+53.5)/27\big) & \text{for } V \leq -10 \\ 2\exp((-V-53.5)/27) & \text{for } V > -10 \end{cases}$$

$$\beta_m(V) = \begin{cases} 2\exp((V+53.5)/27) - \alpha_m(V) & \text{for } V \leq -10 \\ 0 & \text{for } V > -10 \end{cases}$$

The channel kinetics for $I_{\mathrm{K(Ca)}}$ was taken without modification from Traub et al. (2003).

Muscarinic potassium current I_{M}

$$I_{\mathrm{K}} = \bar{g}_{\mathrm{K_M}} n(E_{\mathrm{K_M}} - V)$$

$$\frac{\partial n}{\partial t} = \frac{n_\infty(V)-n}{\tau_n(V)}$$

$$\alpha_n(V) = \frac{0.001(V-30)}{1-\exp(-(V-30)/9)}$$

$$\beta_n(V) = \frac{-0.001(V-30)}{1-\exp((V-30)/9)}$$

$$n_\infty(V) = \frac{\alpha_n(v)}{\alpha_n(V)+\beta_n(V)}$$

$$\tau_{n_{\mathrm{M}}}(V) = \frac{1}{\alpha_n(V)+\beta_n(V)}$$

The values for the rates were adjusted from their original values given at 23°C to 37°C using a Q_{10} of 2.3 (Mainen et al., 1995; Mainen and Sejnowski, 1996).

Medium after hyperpolarization current I_{mAHP}

$$I_{\mathrm{mAHP}} = \bar{g}_{\mathrm{mAHP}} m(E_{\mathrm{mAHP}} - V)$$

$$\frac{\partial m}{\partial t} = \frac{m_\infty(V)-m}{\tau_{m_{\mathrm{mAHP}}}}$$

$$\alpha_m(V) = 0.48\Big/\left(1+\frac{0.18}{[\mathrm{Ca}]_i}\exp(-1.68V\mathcal{F}/R\mathcal{T})\right)$$

$$\beta_m(V) = 0.28\Big/\left(1+\frac{[\mathrm{Ca}]_i}{0.011\exp(-2V\mathcal{F}/R\mathcal{T})}\right)$$

$$m_\infty(V) = \frac{\alpha_m(V)}{\alpha_m(V)+\beta_m(V)}$$

$$\tau_{\mathrm{mAHP}}(V) = \frac{1}{\alpha_m(V)+\beta_m(V)}$$

The medium AHP current was taken without modification from Poirazi et al. (2003a); Poirazi et al. (2003b); Moczydlowski and Latorre (1983) with temperature set to 37°C

Slow afterhyperpolarization current I_{sAHP}

$$I_{\mathrm{sAHP}} = \bar{g}_{\mathrm{sAHP}} m^3(E_{\mathrm{sAHP}} - V)$$

$$\frac{dm}{dt} = \frac{m_\infty([\mathrm{Ca}]_i)-m}{\tau_{\mathrm{sAHP}}([\mathrm{Ca}]_i)}$$

$$m_\infty\big([\mathrm{Ca}]_i\big) = \frac{[\mathrm{Ca}]_i^2}{0.025^2+[\mathrm{Ca}]_i^2}$$

$$\tau_{\mathrm{sAHP}}\big([\mathrm{Ca}]_i\big) = max\left(\frac{1}{0.033\big(1+([\mathrm{Ca}]_i/0.025)^2\big)},0.5\right)$$

The kinetics for the slow AHP current were similar to those used in previous studies where the rates were adjusted from their original values assumed to be given at 22°C to 37°C using a Q_{10} of 3 (Destexhe et al., 1994; Poirazi et al., 2003a,b).

Persistent sodium current $I_{Na(P)}$

$$I_{Na(P)} = \bar{g}_{Na(P)} m(E_{Na(P)} - V)$$

$$\frac{dm}{dt} = \frac{m_\infty - m}{\tau_{m_{Na(P)}}}$$

$$m_\infty(V) = \frac{1}{1+\exp(-(V+48)/10)}$$

$$\tau_{m_{Na(P)}} = 0.025 + 0.14\exp((V+40)/10) \qquad V < -40$$

$$= 0.02 + 0.145\exp(-(V+40)/10) \qquad V \geq -40$$

The kinetics and current description of $I_{Na(P)}$ was taken without modification from Traub et al. (2003).

Reversal potentials used in currents are given as follows: $E_{leak} = -80$ mV, $E_{Na} = E_{Na(P)} = 50$ mV, $E_{Ca(T)} = 140$ mV, $E_{Kdr} = E_{K(A)} = E_{K(Ca)} = E_{mAHP} = E_{sAHP} = -90$ mV, and $E_{K(H)} = -35$ mV. Furthermore, we uniformly shifted the voltage dependence of the sodium, delayed rectifier potassium, N- and T-type voltage-dependent calcium channels, and the activation rate of the L-type calcium by –10, –5, 10, 10, and 8.25 mV, respectively, in order to raise/lower the threshold of sodium/calcium spike generation.

INTRACELLULAR CALCIUM DYNAMICS

Calcium accumulation, extrusion, diffusion and buffering was simulated according to the following simple model which accounts for these processes by a simple exponential decay,

$$\frac{d[\mathrm{Ca}]_i}{dt} = \frac{[\mathrm{Ca}]_\infty - [\mathrm{Ca}]_i}{\tau_{Ca}} + \frac{1}{2\mathcal{F}d}\left(I_{Ca(HVA)} + I_{Ca(T)} + I_{Ca(N)} + I_{Ca(NMDA)}\right)/20$$

where $[\mathrm{Ca}]_\infty$=50 μM is the equilibrium concentration of intracellular calcium, $[\mathrm{Ca}]_i$ denotes the concentration of intracellular free calcium, τ_{Ca} = 20/1.2 ms and τ_{Ca} = 50 ms were the diffusion rate constants respectively used for the dendrite and soma, d is the diameter of the compartment, $I_{Ca(HVA)}$, $I_{Ca(T)}$and $I_{Ca(N)}$ respectively denotes the calcium current through L-type, T-type and N-type calcium channels, and $I_{Ca(NMDA)} = 0.1I_{NMDA}$ is a fractional calcium current through postsynaptic NMDA receptors where 10% of the NMDA-mediated current is carried by calcium (Burnashev et al., 1995; Garaschuk et al., 1996). Synaptic conductances and currents were modeled as follows:

AMPA CONDUCTANCE AND CURRENT

$$g_j^{\mathrm{AMPA}}(t) = \bar{g}^{\mathrm{AMPA}} F w_j(t)\left(\mathrm{e}^{-(t-t_i)/\tau_d^{\mathrm{AMPA}}} - \mathrm{e}^{-(t-t_i)/\tau_o^{\mathrm{AMPA}}}\right)H(t-t_i),$$

$$I_j^{\mathrm{AMPA}}(t) = g_j^{\mathrm{AMPA}}(t)\left(V - E_{\mathrm{rev}}^{\mathrm{AMPA}}\right)$$

$\mathrm{GABA_A}$ CONDUCTANCE AND CURRENT

$$g_j^{\mathrm{GABA_A}}(t) = \bar{g}^{\mathrm{GABA_A}} F\left(\mathrm{e}^{-(t-t_i)/\tau_d^{\mathrm{GABA_A}}} - \mathrm{e}^{-(t-t_i)/\tau_o^{\mathrm{GABA_A}}}\right)H(t-t_i),$$

$$I_j^{\mathrm{GABA_A}}(t) = g_j^{\mathrm{GABA_A}}(t)\left(V - E_{\mathrm{rev}}^{\mathrm{GABA_A}}\right)$$

where $E_{\mathrm{rev}}^{\mathrm{AMPA}} = 0$ mV, $E_{\mathrm{rev}}^{\mathrm{GABA_A}} = -80$ mV, $H(t)$ is the Heaviside step function, w_j denotes the efficacy of the AMPA conductance in synapse j, and F is a normalization factor such that an event with $\bar{g} = 1$ generates a peak conductance of 1 μ*S*. The maximal AMPA $\bar{g}^{\mathrm{AMPA}}$ and $\mathrm{GABA_A}$ $\bar{g}^{\mathrm{GABA_A}}$ conductance were 5 and 2 nS, respectively. Onset and decay time constants were $\tau_o^{\mathrm{AMPA}} = 0.2$ ms and $\tau_d^{\mathrm{AMPA}} = 1.5$ ms for AMPA and $\tau_o^{\mathrm{GABA_A}} = 1.2$ ms and $\tau_d^{\mathrm{GABA_A}} = 9$ ms $\mathrm{GABA_A}$ conductances, respectively. Excitatory AMPA weights were initialized to $w_j(t)$=0.5.

NMDA CONDUCTANCE AND CURRENT

The postsynaptic NMDA conductance was modeled using a simple two state kinetic scheme represented by the following two state diagram

$$C + T \underset{\beta}{\overset{\alpha}{\rightleftharpoons}} O$$

where α and β represent forward and backward voltage independent reaction rates. Defining ζ as the fraction of receptors in the open state of synapse j, then the above two state reaction is described by the following first order kinetic equation:

$$\frac{d\zeta_j}{dt} = \alpha[T](1-\zeta_j) - \beta\zeta_j$$

where α = 10 ms^{-1} and β = 0.0125 ms^{-1} denotes the forward binding and backward unbinding rates, respectively. The concentration $[T]$ denotes a pulse of neurotransmitter of duration 1.1 ms in the synaptic cleft. The NMDA conductance is given by,

$$g_j^{\mathrm{NMDA}}(t) = \bar{g}^{\mathrm{NMDA}}\zeta_j(t)$$

while the NMDA current is,

$$I_j^{\mathrm{NMDA}}(t) = g_j^{\mathrm{NMDA}}(t)B(V)(V - E_{\mathrm{rev}}^{\mathrm{NMDA}})$$

where the reversal potential is $E_{\mathrm{rev}}^{\mathrm{NMDA}} = 0$, and $B(V)$ represents magnesium block described by the following voltage-dependent process,

$$B(V) = \frac{1}{1+\exp(-0.062V)\left[\mathrm{Mg}^{2+}\right]_o/3.57},$$

where the extracellular magnesium concentration was set to a value of $[\mathrm{Mg}^{2+}]_O$ = 1 mM.

$\mathrm{GABA_B}$ CONDUCTANCE AND CURRENT

Post synaptic $\mathrm{GABA_B}$ receptor responses are activated by an intracellular second messenger system, mediated by fast G-protein binding to K^+ channels, whose state diagram is represented by the following kinetic scheme

$$R_o + T \rightleftharpoons R \rightleftharpoons D$$

$$R + G_o \rightleftharpoons RG \rightarrow R + G$$

$$G \rightarrow G_o$$

$$C_1 + nG \rightleftharpoons O$$

The activated and desensitized forms of the receptor G and D respectively arise after neurotransmitter T binds to the receptor R_o. Concurrently, the active form of the G-protein G is produced after the inactive form G_o has been catalyzed by R, and consequently binds to open K^+ channels, with n = 4 binding

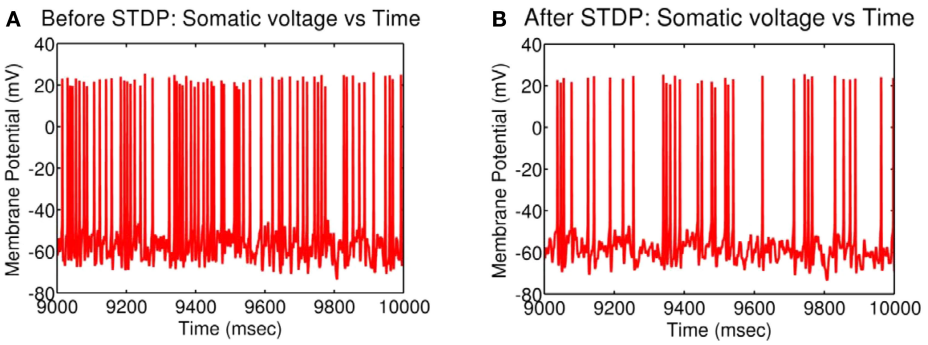

FIGURE S1 | An illustration of how the STDP leads to a decrease in the somatic firing rate. (A) Shows the somatic membrane potential before STDP. **(B)** The somatic membrane potential after STDP.

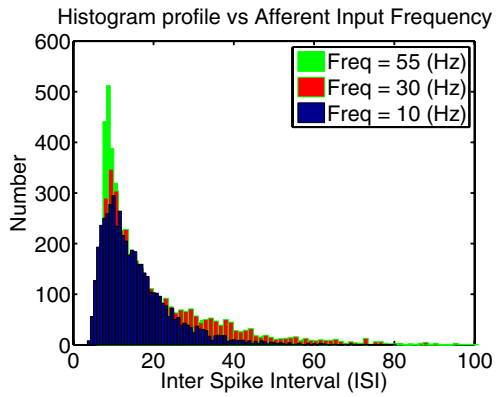

FIGURE S2 | Here we illustrate how increasing the mean input frequency of afferent fiber inputs alters the raw ISI histograms. Note that for increasing values of frequency there is a clear trend where the half width at half maximum (HWHM) of these ISI distributions decreases while the peak count rises.

sites. The above kinetic scheme can be simplified, by assuming Michaelis–Menton kinetics, fast binding to K^+ channels, quasi stationarity of the intermediate enzymatic reactions, no receptor desensitization, and an excess of inactive G-proteins G_o, to the following system,

$$\frac{d[R_j]}{dt} = K_1[T]\left(1-[R_j]\right) - K_2[R_j]$$

$$\frac{d[G_j]}{dt} = K_3[T][R_j] - K_4[G_j]$$

$$g_j^{\mathrm{GABA_B}}(t) = \bar{g}_j^{\mathrm{GABA_B}} \frac{[G(t)]^n}{[G(t)]^n + K_d}$$

$$I_j^{\mathrm{GABA_B}} = g_j^{\mathrm{GABA_B}}(t)\left(V - E_{\mathrm{rev}}^{\mathrm{GABA_B}}\right)$$

where $\bar{g}_j^{\mathrm{GABA_B}}$ is the maximal conductance of $\mathrm{GABA_B}$ receptors, $g_j^{\mathrm{GABA_B}}(t)$ denotes the $\mathrm{GABA_B}$ conductance, K_d is the dissociation constant of G-protein binding to K^+ channels, and $E_{\mathrm{rev}}^{\mathrm{GABA_B}} = -95\,\mathrm{m}V$ is the reversal potential.

The conductance densities $g_{\mathrm{K(H)}}$, $g_{\mathrm{Ca(HVA)}}$, and $g_{\mathrm{Ca(N)}}$ are monotonically increasing functions of distance from the soma to the end of the dendrites. They are respectively given as follows:

$$g_{\mathrm{K(H)}}(x) = \bar{g}_{\mathrm{K(H)}}^{\mathrm{soma}} + \frac{\left(\bar{g}_{\mathrm{K(H)}}^{\mathrm{end}} - \bar{g}_{\mathrm{K(H)}}^{\mathrm{soma}}\right)}{1+\exp\left(\left(d_{\frac{1}{2}} - 0.75[x-100]_+\right)/100\right)},$$

where $\bar{g}_{\mathrm{K(H)}}^{\mathrm{soma}} = 0$ and $\bar{g}_{\mathrm{K(H)}}^{\mathrm{end}} = 12.5\,pS/\mu m^2$.

$$g_{\mathrm{Ca(HVA)}}(x) = \bar{g}_{\mathrm{Ca(HVA)}}^{\mathrm{soma}} + \frac{\left(\bar{g}_{\mathrm{Ca(HVA)}}^{\mathrm{end}} - \bar{g}_{\mathrm{Ca(HVA)}}^{\mathrm{soma}}\right)}{1+\exp\left(\left(d_{\frac{1}{2}} - [x-100]_+\right)/25\right)},$$

where $\bar{g}_{\mathrm{Ca(HVA)}}^{\mathrm{soma}} = 10$ and $\bar{g}_{\mathrm{Ca(HVA)}}^{\mathrm{end}} = 60\ \mathrm{pS}/\mu\mathrm{m}^2$.

$$g_{\mathrm{Ca(N)}}(x) = \bar{g}_{\mathrm{Ca(N)}}^{\mathrm{soma}} + \frac{\left(\bar{g}_{\mathrm{Ca(N)}}^{\mathrm{end}} - \bar{g}_{\mathrm{Ca(N)}}^{\mathrm{soma}}\right)}{1+\exp\left(\left(d_{\frac{1}{2}} - x\right)/50\right)},$$

where $\bar{g}_{\mathrm{Ca(N)}}^{\mathrm{soma}} = 0$, $\bar{g}_{\mathrm{Ca(N)}}^{\mathrm{end}} = 12.5\,pS/\mu m^2$, $d_{1/2}$ is half the maximal path distance from the soma to the end of the longest dendrite, and $[\cdot]_+$ stands for rectification.

STDP CAN REDUCES SOMATIC FIRING RATE

Here, we illustrate changes in the somatic firing rate of the model neuron before and after STDP. In this case the initial weights of the AMPA conductances were initialized to $w_j(t) = 0.1$. **Figure S1A** shows that before STDP, the soma generates spikes at a high rate, however in **Figure S1B**, the somatic firing rate has clearly reduced after STDP.

FREQUENCY ALTERS ISI HISTOGRAM PROFILES

Increasing the mean input frequency of afferent inputs leads to observable changes in the ISI distribution of the soma as seen in **Figure S2**. There is a clear tendency for increasing input frequencies to give rise to increases in the peak of the ISI distribution. Additionally, there is also an increase the ISI histogram's length of the tail.

REFERENCES

Burnashev, N., Zhou, Z., Neher, E., and Sakmann, B. (1995). Fractional calcium currents through recombinant GLUR channels of the NMDA, AMPA and kainate receptor subtypes. *J. Physiol.* 485.2, 403–418.

Destexhe, A., Contreras, D., Sejnowski, T. J., and Steriade, M. (1994). A model of spindle rhythmicity in the isolated thalamic reticular nucleus. *J. Neurophysiol.* 72, 803–818.

Garaschuk, O., Schneggenburger, R., Schirra, C., Tempia, F., and Konnerth, A. (1996). Fractional CA2+ currents through somatic and dendritic glutamate receptor channels of rat hippocampal CA1 pyramidal neurones. *J. Physiol.* 485.2, 403–418.

Kampa, B. M., Letzkus, J. J., and Stuart, G. J. (2006). Requirement of dendritic calcium spikes for induction of spike-timing-dependent synaptic plasticity. *J. Physiol.* 574.1, 283–290.

Kampa, B. M., and Stuart, G. J. (2006). Calcium spikes in basal dendrites of layer 5 pyramidal neurons during action potential bursts. *J. Neurosci.* 26, 7424–7432.

Larkum, M. E., Waters, J., Sakmann, B., and Helmchen, F. (2007). Dendritic spikes in apical dendrites of neocortical layer 2/3 pyramidal neurons. *J. Neurosci.* 27, 8999–9008.

Lazarewicz, M. T., Migliore, M., and Ascoli, G. A. (2002). A new bursting model of CA3 pyramidal cell physiology suggests multiple locations for spike initiation. *Biosystems* 67, 129–137.

Mainen, Z. F., Joerges, J., Huguenard, J. R., and Sejnowski, T. J. (1995). A model of spike initiation in neocortical pyramidal cells. *Neuron* 15, 1427–1439.

Mainen, Z. F., and Sejnowski, T. J. (1996). Influence of dendritic structure on firing pattern in model neocortical neurons. *Nature* 382, 363–366.

Moczydlowski, E., and Latorre, R. (1983). Gating kinetics of Ca2+-activated K+ channels from rat muscle incorporated into planar lipid bilayers. Evidence for two voltage-dependent Ca2+ binding reactions. *J. Gen. Physiol.* 82, 511–542.

Poirazi, P., Brannon, T., and Mel, B. W. (2003a). Arithmetic of subthreshold synaptic summation in a model CA1 pyramidal cell, *Neuron* 37, 977–987.

Poirazi, P., Brannon, T., and Mel, B. W. (2003b). Pyramidal neuron as a two-layer neural network. *Neuron* 37, 989–999.

Rhodes, P. A., and Gray, C. M. (1994). Simulations of intrinsically bursting neocortical pyramidal neurons. *Neural Comput.* 6, 1086–1110.

Rhodes, P. A., and Llinás, R. R. (2001). Apical tuft input efficacy in layer 5 pyramidal cells from rat visual cortex. *J. Physiol.* 6, 1086–1110.

Traub, R. D., Buhl, E. H., Gloveli, T., and Whittington, M. A. (2003). Fast rhythmic bursting can be induced in a layer 2/3 cortical neurons by enhancing persistent Na^+ conductance or by blocking BK channels. *J. Neurophysiol.* 89, 909–921.

Zhou, F.-M., and Hablitz, J. J. (1996). Layer I neurons of rat neocortex. II. voltage-dependent outward currents. *J. Neurophysiol.* 76, 668–682.